Biochemical Pharmacology 77 (2009) 1418–1428

Contents lists available at ScienceDirect

Biochemical Pharmacology

journal homepage: www.elsevier.com/locate/biochempharm

Identification of metabolites of meisoindigo in rat, pig and human liver microsomes by UFLC–MS/MS

Meng Huang, Paul C. Ho *

Department of Pharmacy, Faculty of Science, National University of Singapore, 117543, Singapore

ARTICLE INFO

Article history:
Received 29 December 2008
Accepted 20 January 2009

Keywords:
In vitro metabolism
Meisoindigo
Liver microsomes
Interspecies differences
UFLC–MS/MS

ABSTRACT

3-(1,2-Dihydro-2-oxo-3H-indol-3-ylidene)-1,3-dihydro-1-methyl-2H-indol-2-one, abbreviated as meisoindigo, has been a routine therapeutic agent in the clinical treatment of chronic myelogenous leukemia in China since the 1980s. To gain an understanding of the interspecies differences in the metabolism of meisoindigo, the relevant metabolism studies were carried out for the first time in rat, pig and human liver microsomes of different genders by ultra fast liquid chromatography/tandem mass spectrometry (UFLC–MS/MS). The qualitative metabolite identification was accomplished by multiple reaction monitoring (MRM) in combination with Enhanced Product Ion (EPI). The semi-quantitative metabolic stability and metabolite formation were simultaneously measured by MRM. The *in vitro* metabolic pathways of meisoindigo in three species were proposed as 3,3′ double bond reduction, followed by N-demethylation, and reduction followed by phenyl mono-oxidation. Two novel metabolic pathways involving direct phenyl mono-oxidation without reduction in the three species, and direct N-demethylation without reduction in only pig and human, were also proposed. It may be noted that the two metabolites formed after reduction followed by phenyl mono-oxidation at positions 4, 5, 6 or 7, as well as one metabolite formed from direct phenyl mono-oxidation at either of the two phenyl rings without reduction were found to be uniquely present in human. The *in vitro* $t_{1/2}$ and *in vitro* CL_{int} values of meisoindigo were calculated. Statistical analysis showed there were no significant differences in the metabolic stability profiles of meisoindigo among three species, and gender effect on the metabolic stability of meisoindigo was negligible. Formation profiles of the most significant reductive metabolites were obtained in the three species.

1. Introduction

Meisoindigo, a synthetic derivative of indirubin, has been a routine therapeutic agent in the clinical treatment of chronic myelogenous leukemia (CML) in China since the 1980s [1–3]. In order to improve the understanding of its efficacy and safety characteristics, investigation of meisoindigo metabolism in animals or humans plays a critical role. However, information relevant to *in vitro* metabolism of meisoindigo is limited so far. A preliminary study was reported on metabolism of meisoindigo in male rat liver microsomes by reversed-phase high performance liquid chromatography (RP-HPLC) with diode array detector (DAD) [4]. In our previous study, *in vitro* stereoisomeric metabolites of meisoindigo with the substrate concentration of 50 μM in male rat liver microsomes were identified by achiral and chiral liquid chromatography/tandem mass spectrometry (LC–MS/MS), together with proton NMR spectroscopy and synchrotron infrared spectroscopy. Three parallel metabolic pathways of meisoindigo in male rat liver microsomes were thereby proposed as direct 3,3′ double bond reduction, reduction followed by N-demethylation, as well as reduction followed by phenyl mono-oxidation [5]. Although the use of Enhanced Q3 Single MS (EMS) in combination with Enhanced Product Ion (EPI) led to considerably successful metabolite detection and structural elucidation in our previous study, the approach is disadvantaged by the limited detection sensitivity of the full scan mode due to the high background signal from the microsomal matrices. The search for metabolites using precursor ion (PI) scan and neutral loss (NL) scan shows a relatively high sensitivity but assumes that the metabolites have a common fragment with the parent drug. Unfortunately, based on our previous results, the metabolites of meisoindigo at *m/z* 279, 265, 295 all underwent 3,3′ double bond reduction of the parent drug, thus resulting in distinct fragmentation mechanisms from that of the parent drug. Hence, characteristic fragment ions could not be identified for the PI or NL scan. Considering a hybrid triple

* Corresponding author. Tel.: +65 6516 2651; fax: +65 6779 1554.
E-mail address: phahocl@nus.edu.sg (P.C. Ho).

Abbreviations: CML, chronic myelogenous leukemia; UFLC, ultra fast liquid chromatography; MS, mass spectrometry; MS/MS, tandem mass spectrometry; QTRAP, hybrid triple quadrupole linear ion trap; MRM, multiple reaction monitoring; EPI, Enhanced Product Ion.

0006-2952/$ – see front matter © 2009 Elsevier Inc. All rights reserved.
doi:10.1016/j.bcp.2009.01.012

quadrupole linear ion trap (QTRAP) set to perform multiple reaction monitoring (MRM) offers high sensitivity, selectivity, and a good dynamic range, MRM screening could be an alternative approach for metabolite detection, especially for the minor metabolites with trace amounts. Besides, MRM could be used to carry out simultaneous quantitative analysis of the parent drug disappearance and metabolite appearance in liver microsomes across multiple species. With appropriate dwell time and fixed number of MRM transitions, relative quantification could be achieved attributed to the fast scanning capability of the hybrid triple quadrupole linear ion trap under the linear ion trap mode that enabled enough data points to be collected across the chromatographic peaks for quantification. A higher number of data points for a chromatographic peak also provided reproducible peak areas for quantification purposes [6].

On the other hand, stereoisomeric reductive plus phenyl mono-oxidative metabolites at *m/z* 295 were speculated to be very close chromatographic peaks due to tiny chromatographic profile differences, caused by different position of OH group on either of the two phenyl rings, as well as the different absolute configurations at positions 3 and 3′ [5]. Considering ultra fast liquid chromatography (UFLC) has the capability in higher chromatographic resolution through smaller particle packing column material (2.2 μm) and higher pressure pumps as compared to conventional HPLC, UFLC could be utilized to screen out more stereoisomeric reductive plus phenyl mono-oxidative metabolites at *m/z* 295, or even other types of minor metabolites of meisoindigo.

In view of interspecies variability as an important internal factor affecting drug metabolism, the purpose of the present study was to qualitatively and quantitatively investigate the *in vitro* metabolism of meisoindigo in liver microsomes from three species rat, pig and human of different genders utilizing UFLC coupled with QTRAP, and establish the metabolic profiles in terms of metabolite identification, metabolic stability, metabolite formation and gender effect. Identification of the phase I metabolites and the semi-quantitative analysis of the parent disappearance as well as the corresponding metabolite formation along the incubation time in liver microsomes of male and female rats, pigs, and humans, were conducted by monitoring MRM transitions at the relevant therapeutic concentration levels of 50 μM and 1 μM, respectively [7]. Responses of the parent and the metabolites were plotted along the incubation time for the three species, and the differences among species are subsequently identified.

2. Materials and methods

2.1. Chemicals

All chemicals were of analytical grade and used without further purification. Meisoindigo was provided by Institute of Materia Medica, Chinese Academy of Medical Sciences and Peking Union Medical College, Beijing, China. Bradford reagent, bovine serum albumin (BSA), formic acid and β-NADPH were purchased from Sigma Chemical Co. (St. Louis, Mo, USA). HPLC grade methanol and acetonitrile were purchased from Fisher Scientific Co. (Fair Lawn, NY, USA). Milli-Q water was obtained from a Millipore water purification system (Billerica, MA, USA) and used to prepare buffer solutions and other aqueous solutions.

2.2. Liver microsomal preparation and origin

Pooled different gender rat and pig liver microsomes were prepared according to the method reported previously [8]. Three male and three female Sprague–Dawley (SD) rats were obtained from Animal Holding Unit, National University of Singapore. Three male and three female Large White-Landrace-Duroc pigs were obtained from Buroh Lane Abattoir, Primary Industries Pte Ltd, Singapore. Rats were euthanized with CO_2 after a 24-h fasting period. Pigs were slaughtered by electric shock at the abattoir. The pooled extracted liver microsomes were suspended in 0.1 M Tris buffer (pH 7.4) and stored at −80 °C before use. The rat and pig microsomal protein contents were determined by Bradford assay method, using BSA as the standard protein [9]. Pooled male human liver microsomes from 10 individuals and pooled female human liver microsomes from 10 individuals were both purchased from BD Gentest™ (Woburn, MA, USA). The human microsomal protein contents were 20 mg/ml.

2.3. Liver microsomal incubations

Meisoindigo stock solution in methanol was added to 0.1 M Tris buffer (pH 7.4) with rat, pig or human liver microsomes respectively. The mixture was first shaken for 5 min for equilibration in a shaking water bath at 37 °C. The incubation was then initiated by adding β-NADPH solution. The final concentrations of meisoindigo, NADPH and the microsomal protein were 50 μM, 1 mM and 1 mg/mL, respectively in a typical incubation mixture (1 mL) for metabolite identification study. The final concentrations of meisoindigo, NADPH and the microsomal protein were 1 μM, 1 mM and 0.5 mg/mL, respectively in a typical incubation mixture (1 mL) for metabolic stability and metabolite formation studies. The percentage of methanol in the incubation mixture was kept less than 1% (v/v). For metabolite identification study, samples were incubated for 60 min. For metabolic stability and metabolite formation studies, aliquots of 100 μL of the incubation sample mixtures were collected at 5, 10, 20, 30, 40, 50, 60 and 90 min. The reaction was terminated with the same volume of ice-cold acetonitrile to precipitate proteins and the samples were subsequently centrifuged at 16,000 × *g* for 15 min. Negative controls were prepared with NADPH added followed by immediate termination using ice-cold acetonitrile and set as the 0 min aliquots. All experiments were carried out in triplicate. A 5 μL supernatant was taken and analyzed by UFLC–MS/MS.

2.4. UFLC–MS/MS analysis

The controls and samples were analyzed on a Q TRAP™ 3200 MS/MS system from Applied Biosystems/MDS Sciex (Concord, Ontario, Canada) coupled to a Prominence™ UFLC system (Shimadzu, Japan). Separations were accomplished on a Shim-pack XR-ODS column (50 mm × 3.0 mm, 2.2 μm) (Shimadzu, Japan) with a guard cartridge at temperature of 80 °C. The mobile phase consisted of 0.1% formic acid in water (solvent A) and acetonitrile (solvent B) and was delivered at a flow rate of 0.8 mL/min. The linear gradient elution program was as follows: 5–95% B over 14 min, followed by an isocratic hold at 95% B for another 1 min. At 15 min, B was returned to 5% in 0.1 min and the column was equilibrated for 4.9 min before the next injection. The total run time for each injection was 20 min. The mass spectrometer was operated in the positive ion mode with a TurboIonSpray source. A list of 9 MRM transitions with the addition of parent drug in Table 1 was used to cover the most common phase I biotransformation reactions of meisoindigo. The Q1, Q3, declustering potential (DP), and collision energy (CE) values were based on the phase I biotransformation prediction of meisoindigo by MetaboliteID 1.4 software from Applied Biosystems/MDS Sciex as well as the previous EMS and EPI results of meisoindigo and its phase I metabolites [5]. The other ionization parameters were as follows: curtain gas (CUR), 30 (arbitrary units); ion source gas 1 (GS1), 40 (arbitrary units); ion source gas 2 (GS2), 50 (arbitrary units); source temperature (TEM), 650 °C; entrance potential (EP), 10 V.

Table 1
MRM transition parameters for meisoindigo and its *in vitro* metabolites.

Biotransformation	Mass gain/loss (amu)	Q1 (amu)	Q3 (amu)	DP (V)	CE (eV)
Parent	0	277.1	234.2	66	45
Hydrogenation	2	279.1	147.1	60	30
Hydrogenation + demethylation	−12	265.1	133.1	60	30
Hydrogenation+oxidation	18	295.1	163.1	60	30
Hydrogenation + oxidation	18	295.1	147.1	60	30
Oxidation	16	293.1	249.1	60	40
Dioxidation	32	309.1	265.1	60	40
Demethylation	−14	263.1	235.1	60	40
Hydrogenation + dioxidation	34	311.1	178.1	60	30

The dwell time of each MRM transition was 150 ms. The mass spectrometer and the UFLC system were controlled by Analyst 1.4.2 software from Applied Biosystems/MDS Sciex.

2.5. Metabolite identification

The strongest MRM signals with ion counts higher than 300 were selected. The associated EPI scans were subsequently triggered, ranging from m/z 50 to 300 at a scan rate of 4000 amu/s with dynamic fill in the linear ion trap. The CE value was set at 40 eV with a spread of 5 eV. The search for meisoindigo metabolites was performed manually by interpretation of MRM chromatograms and EPI spectra. The corresponding EPI of potential metabolites were compared with that of meisoindigo to investigate the fragmentation patterns and obtain information on the metabolite structures. The phase I biotransformations predicted by MetaboliteID 1.4 software were also confirmed by the EPI spectra.

2.6. Metabolic stability calculations and statistical analysis

The corresponding MRM transition of meisoindigo was selected and used for peak configuration in Analyst 1.4.2 for semi-quantitation. In the determination of the *in vitro* half-life ($t_{1/2}$), the peak areas of meisoindigo were converted to parent remaining percentages, using the $t = 0$ peak area values as 100%. The parent remaining percentages of meisoindigo were plotted against the microsomal incubation time using Microsoft Excel. Data points were the average of three measurements with standard deviations as the error bars. The *in vitro* $t_{1/2}$ (in units of min) was calculated from the slope of the linear regression of the natural logarithm of the parent remaining percentage versus incubation time according to the following formula [10,11].

$$t_{1/2} = \frac{\ln 2}{\text{slope}}$$

In vitro intrinsic clearance (CL_{int}) (in units of ml/min/kg) was calculated from the $t_{1/2}$ value according to the following formula [10,11].

$$CL_{int} = \frac{\ln 2}{t_{1/2}} \cdot \frac{\text{g liver weight}}{\text{kg body weight}} \cdot \frac{\text{ml incubation}}{\text{mg microsomal protein}} \cdot \frac{\text{mg microsomal protein}}{\text{g liver weight}}$$

It was assumed that rats and humans have 40 and 25.7 g of liver per kg body weight, respectively [12]. Microsomal protein content of the livers was assumed to be 45 and 52.5 mg of microsomal protein per g of liver for rats [13] and humans [14], respectively. Microsomal protein content of the incubation was set as 0.5 mg of microsomal protein per mL of inbubation for both rats and humans as described above.

Statistical comparisons in the rates of meisoindigo metabolism among three species were made using one way analysis of variance (ANOVA) by GraphPad Prism 4 software. Independent two sample t-tests were performed to evaluate the metabolism differences caused by genders. Differences were considered as statistically significant when p value was less than 0.05.

2.7. Metabolite formation

The corresponding MRM transitions of meisoindigo metabolites were selected and used for peak configuration in Analyst 1.4.2 for semi-quantitation. Peak areas of metabolites were calculated and plotted against the microsomal incubation time using Microsoft Excel. Data points were the average of three measurements with standard deviations as the error bars.

3. Results

3.1. Metabolite identification

Table 2 outlines the metabolites of meisoindigo generated in male rat, pig and human microsomes after incubation for 60 min with substrate concentration of 50 μM. Significant metabolites were searched out with the following six MRM transitions except 309.1 → 265.1 and 311.1 → 178.1 (data not shown). Female metabolite profiles were found to be similar as their corresponding

Table 2
Meisoindigo metabolites found in liver microsomes from the three male species after incubation with substrate concentration of 50 μM for 60 min.

Metabolite	MRM transition	Retention time (min)	Rat	Pig	Human
M279-1	279.1 → 147.1	4.34	✓	✓	✓
M279-2		4.92	✓	✓	✓
M265-1	265.1 → 133.1	3.25	✓	✓	✓
M265-2		4.27	✓	✓	✓
M295-1	295.1 → 163.1	3.08	✓	–	–
M295-2		3.16	✓	–	–
M295-3		3.24	✓	✓	✓
M295-4		3.34	✓	–	–
M295-5		3.89	✓	✓	✓
M295-6		4.87	–	–	✓
M295-7		5.05	–	–	✓
M295-8		6.15	✓	–	✓
M295-9	295.1 → 147.1	2.50	✓	–	✓
M295-10		2.93	✓	✓	✓
M295-11		3.04	✓	✓	✓
M295-12		3.56	✓	✓	✓
M295-13		4.21	✓	✓	✓
M295-14		4.86	✓	✓	✓
M295-15		5.06	✓	✓	✓
M295-16		5.28	✓	–	✓
M293-1	293.1 → 249.1	4.87	✓	✓	✓
M293-2		5.08	–	–	✓
M293-3		5.28	✓	✓	–
M293-4		5.44	–	✓	✓
M293-5		5.71	✓	✓	✓
M263	263.1 → 235.1	4.79	–	✓	✓

(✓) metabolite detected; (–) metabolite not detected.

male ones for the same species, while showed lower peak abundances (data not shown).

3.1.1. MRM transition 279.1 → 147.1 and 265.1 → 133.1

All of the three species gave rise to two reductive metabolite isomers i.e. M279-1 and M279-2 with retention times of 4.34 min and 4.92 min, as well as reductive plus N-demethyl metabolite isomers i.e. M265-1 and M265-2 with retention times of 3.25 min and 4.27 min (Table 2). The abundances of these two types of metabolites in rat liver microsomes were much higher than those in the other two liver microsomes, whereas the abundances of these metabolites in pig and human liver microsomes were comparable (data not shown). The proposed fragmentation scheme and MS/MS spectrum of these two types of metabolites were reported in our previous paper [5].

3.1.2. MRM transition 295.1 → 163.1

Six, two and five reductive plus phenyl mono-oxidative (at positions 4, 5, 6 or 7) metabolite isomers were generated in rat, pig and human liver microsomes, respectively (Table 2). Among them, M295-3 (3.24 min) and M295-5 (3.89 min) were observed in all of the three species. M295-1 (3.08 min), M295-2 (3.16 min) and M295-4 (3.34 min) were only observed in rat liver microsomes, whereas M295-6 (4.87 min) and M295-7 (5.05 min) were only observed in human liver microsomes, and not in the other two animal microsomes. The abundances of the common metabolites in all three species were comparable, whereas the two human unique metabolites showed relative low abundances (Fig. 1). The proposed fragmentation scheme and MS/MS spectrum of this type of metabolites were reported in our previous paper [5].

3.1.3. MRM transition 295.1 → 147.1

Eight, six and eight reductive plus phenyl mono-oxidative (at positions 4′, 5′, 6′ or 7′) metabolite isomers were generated in rat, pig and human liver microsomes, respectively (Table 2). Among them, six common metabolites were observed in all of the three species, whereas M295-9 (2.50 min) and M295-16 (5.28 min) were only observed in rat and human liver microsomes rather than pig liver microsomes. The abundances of the common metabolites in all of the three species were distinct, especially the two major metabolites in human liver microsomes i.e. M295-14 (4.86 min) and M295-15 (5.06 min) showed relative high abundances as compared to the other two animal species (Fig. 2). The proposed fragmentation scheme and MS/MS spectrum of this type of metabolites were reported in our previous paper [5].

3.1.4. MRM transition 293.1 → 249.1

Three, four and four phenyl mono-oxidative metabolite isomers were generated in rat, pig and human liver microsomes, respectively (Table 2). Among them, M293-1 (4.87 min) and M293-5 (5.71 min) were observed in all of the three species. M293-3 (5.28 min) was only observed in rat and pig liver microsomes, whereas M293-4 (5.44 min) was only observed in pig and human liver microsomes. Additionally, M293-2 (5.08 min) with very low abundance was only observed in human liver microsomes rather than the other two animal microsomes. The abundances of phenyl mono-oxidative metabolites in pig liver microsomes were more significant than those in the other two liver microsomes (data not shown).

There were two types of EPI (MS/MS) mass spectra with regard to phenyl mono-oxidative metabolites. The result indicated that the two types of metabolites should be position isomers with single hydroxyl group located at the two different phenyl rings. For each type, there were four maximal possibilities regarding the specific positions of hydroxyl group on the phenyl ring. The representative mass spectrum of one type was the EPI of M293-4 (5.44 min). The proposed fragmentation scheme and MS/MS spectrum of this type are shown in Fig. 3(A). Loss of CH_3, H_2O and CO following gain of one H generated the product ion at m/z 278, 275 and 265, respectively. Loss of CONH generated the product ion at m/z 249. Loss of $CONCH_3$ following loss of one H generated the product ion at m/z 234. Loss of both CONH and CO following gain of one H generated the product ion at m/z 222. Loss of CH_3, H_2O, CONH and O following gain of one H generated the product ion at m/z 201. Subsequent loss of CO at position 2 after the cleavage of the 3,3′ bond generated the product ion at m/z 133, which was 16 Da higher than the corresponding product ion of meisoindigo at m/z 117, thus indicating hydroxylation had occurred at one of the positions 4, 5, 6 and 7. Simultaneous cleavages of 1,8 bond and 3,9 bond following loss of one H generated the product ion at m/z 91. The representative of the other type was the EPI of M293-5 (5.71 min). The proposed fragmentation scheme and MS/MS spectrum of this type are shown in Fig. 3(B). The fragmentations of the product ions at m/z 278, 275, 265, 249, 234, 222 and 201 were the same as described above. Subsequent loss of CO at position 2′ after the cleavage of the 3,3′ bond following gain of one H generated the product ion at m/z 120, which was 16 Da higher than the corresponding product ion of meisoindigo at m/z 104, thus indicating hydroxylation had occurred at one of the positions 4′, 5′, 6′ and 7′. Simultaneous cleavages of 1′,8′ bond and 3′,9′ bond following loss of one H generated the product ion at m/z 91.

3.1.5. MRM transition 263.1 → 235.1

Only one N-demethyl metabolite with retention time of 4.79 min was generated in pig and human liver microsomes, while none was found in rat liver microsome incubations (Table 2). The abundance of this metabolite in pig liver microsomes was higher than that in the human liver microsomes (data not shown). The proposed fragmentation scheme and EPI (MS/MS) spectrum of protonated metabolites at m/z 263 are shown in Fig. 4. Loss of H_2O following gain of one H generated the product ion at m/z 245, and subsequent loss of CO generated the product ion at m/z 217. Loss of one or two CO following gain of one H generated the product ions at m/z 235 and m/z 207, respectively. Loss of CONH following gain of one H generated the product ion at m/z 220. Loss of both CONH and CO following gain of one H generated the product ion at m/z 192.

Therefore, based on the metabolite profiling, four metabolic pathways of meisoindigo in the liver microsomes of all three species were proposed as direct 3,3′ double bond reduction, reduction followed by N-demethylation, reduction followed by phenyl mono-oxidation and direct phenyl mono-oxidation (Fig. 5). Among them, direct 3,3′ double bond reduction was the major metabolic pathway for all of the three species. In addition, direct N-demethylation was proposed as a minor metabolic pathway in pig and human liver microsomes that was absent in rat liver microsomes (Fig. 5).

3.2. Metabolic stability

Metabolic stability of meisoindigo was determined in triplicate at eight time points between 5 and 90 min in gender-specific rat, pig and human liver microsomes. Fig. 6(A through C) shows the phase I metabolic stability for meisoindigo in both genders for rat, pig and human liver microsomes, respectively. The error bars reflect the difference of the individual values from the mean. These data indicate that meisoindigo underwent a rapid and extensive metabolism in both genders of all three species. Under the same incubation conditions, about 11%, 18% and 6% of the starting concentration of meisoindigo remained in each gender of rat, pig and human liver microsomes respectively after 90 min of

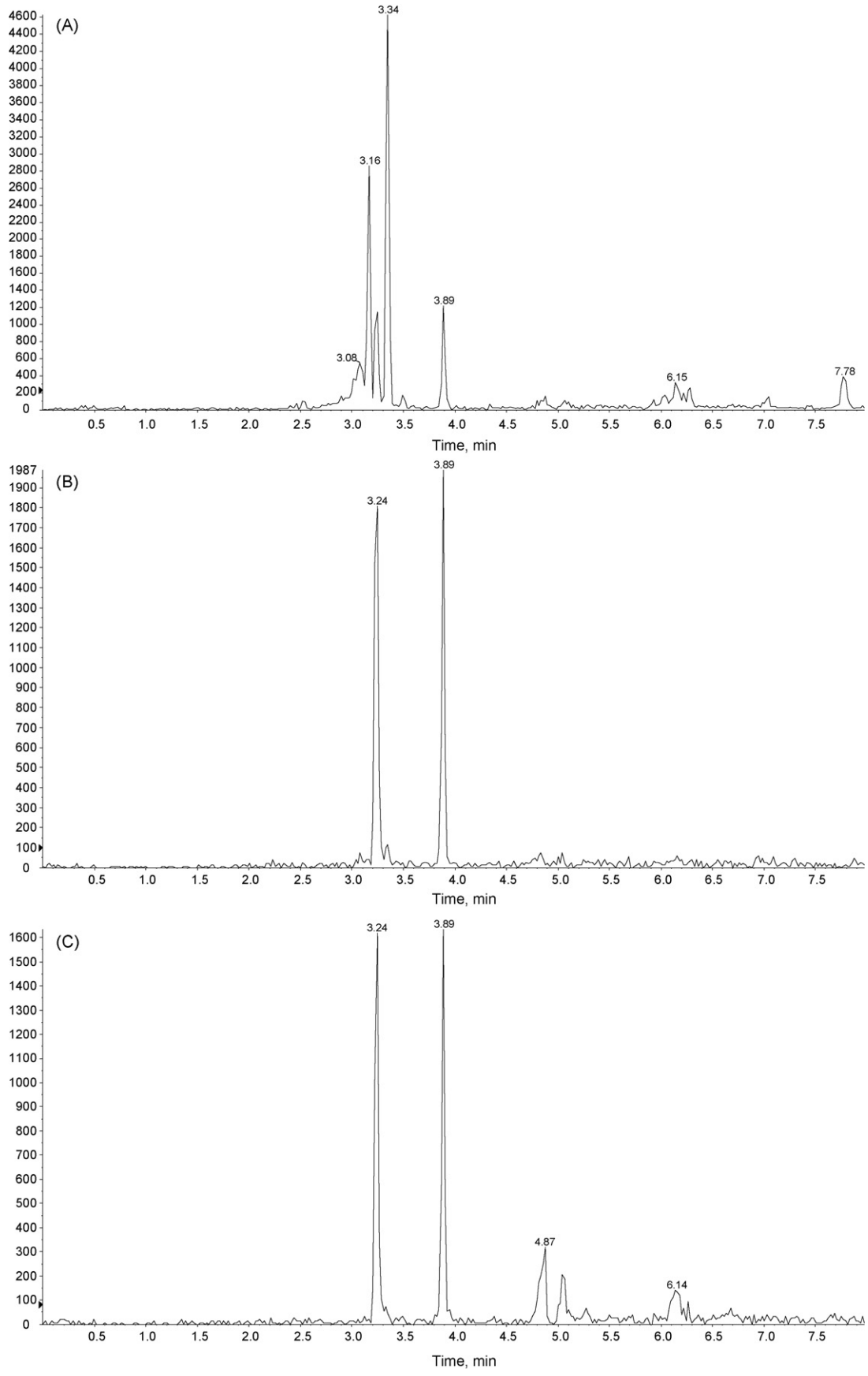

Fig. 1. Extracted ion chromatograms of MRM transition (295.1 → 163.1) for meisoindigo metabolites in liver microsomes: male rat (A), male pig (B), and male human (C).

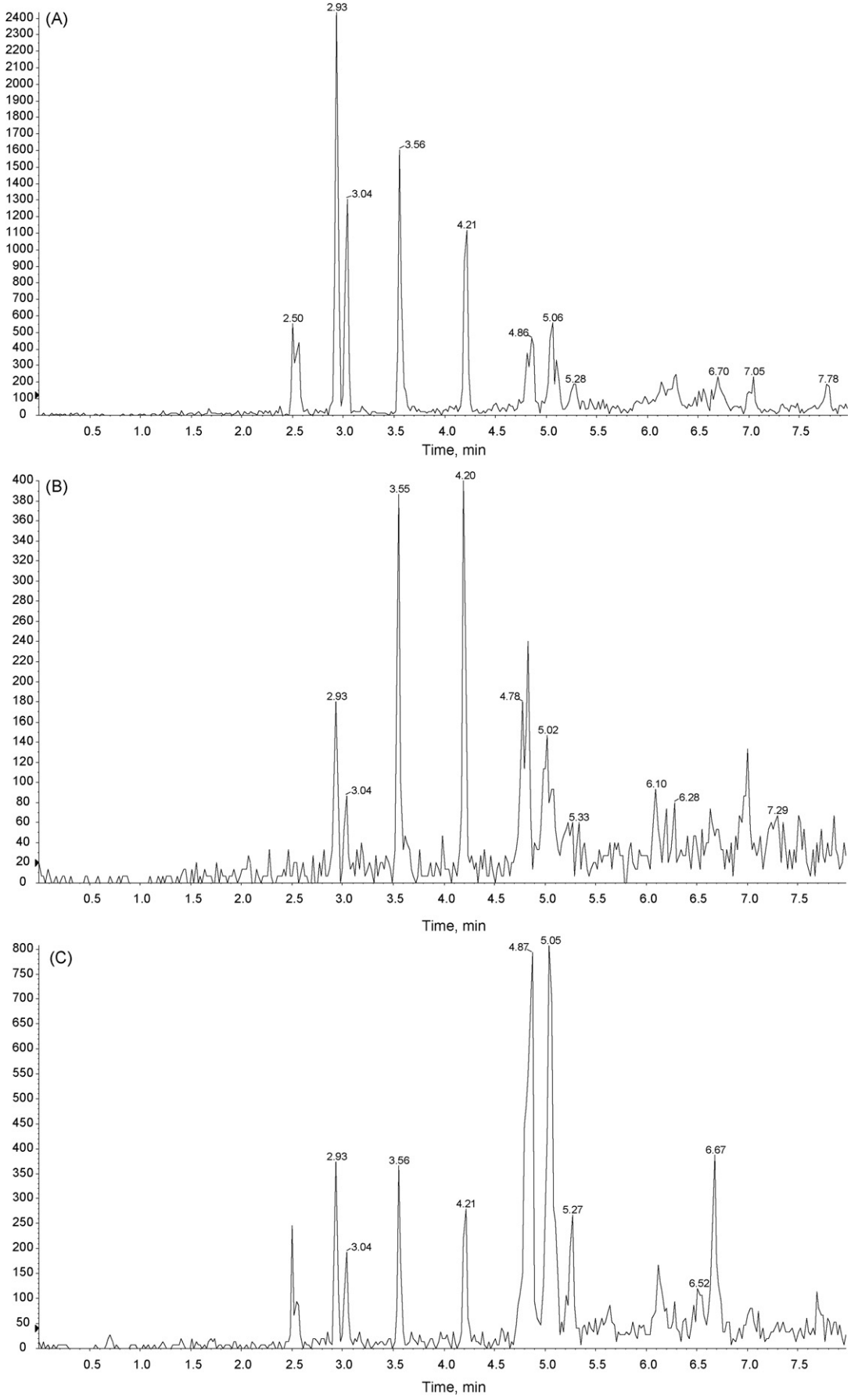

Fig. 2. Extracted ion chromatograms of MRM transition (295.1 → 147.1) for meisoindigo metabolites in liver microsomes: male rat (A), male pig (B), and male human (C).

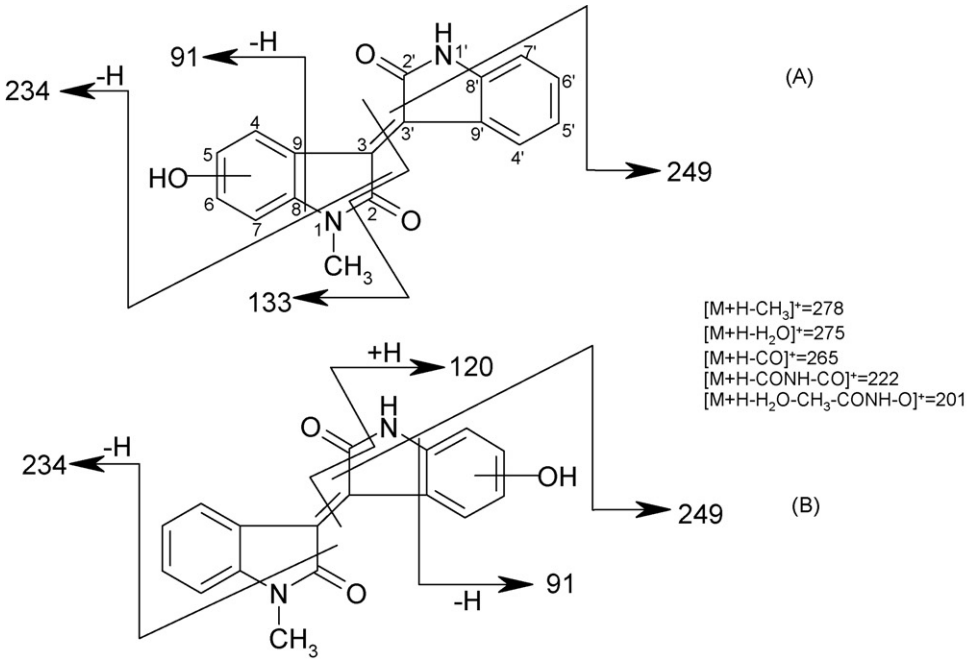

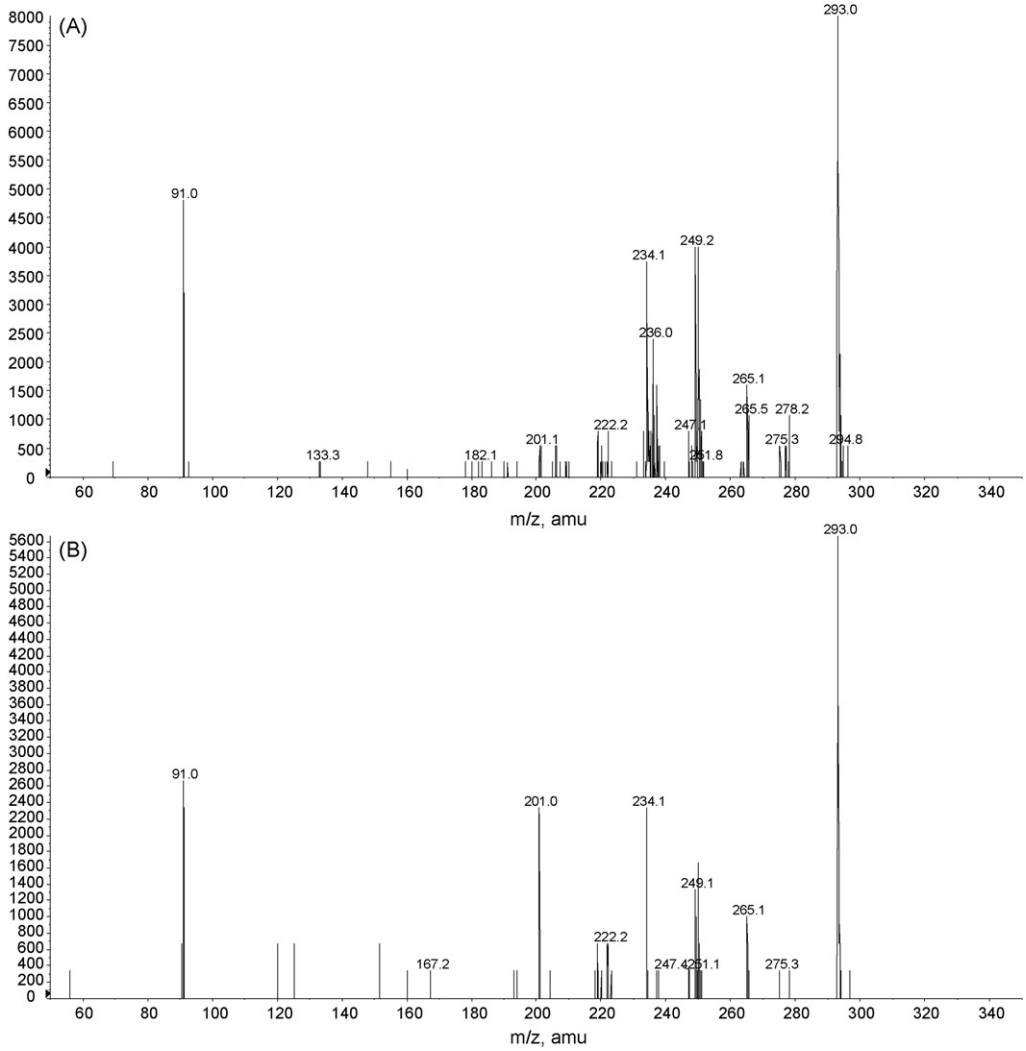

Fig. 3. MS/MS spectra of protonated metabolites at *m*/*z* 293 and the proposed origin of key product ions.

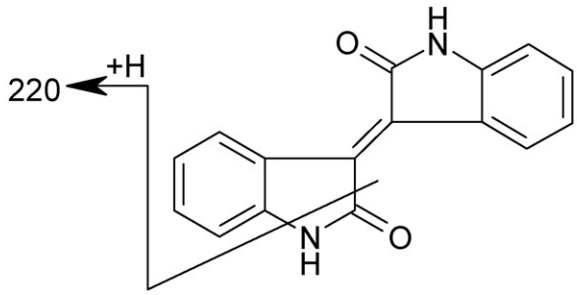

$[M+H-H_2O]^+=245$
$[M+H-CO]^+=235$
$[M+H-H_2O-CO]^+=217$
$[M+H-CO-CO]^+=207$
$[M+H-CONH-CO]^+=192$

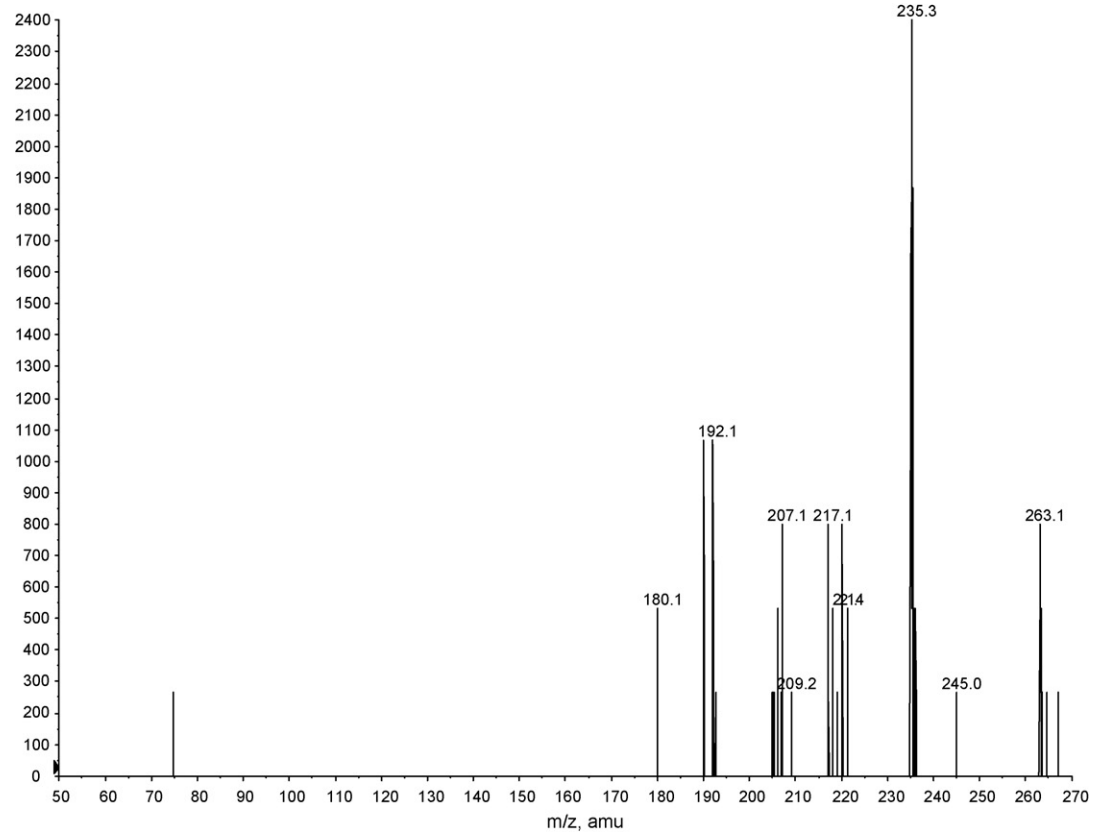

Fig. 4. MS/MS spectrum of the protonated metabolite at *m*/*z* 263 and the proposed origin of key product ions.

incubation. The calculated *in vitro* $t_{1/2}$ and *in vitro* CL_{int} values of meisoindigo in gender-specific rat, pig and human liver microsomes were listed in Table 3, except the *in vitro* CL_{int} values in pig liver microsomes due to the absence of the required physiological parameters in the previous literatures for the pigs used in this study. One way ANOVA analysis showed that there were no statistically significant differences in the rates of meisoindigo metabolism among three species, thus indicating the correlation in the *in vitro* metabolism of meisoindigo in human and the two preclinical animal species, i.e. rats and pigs. Independent two sample *t*-tests showed that there were no statistically significant differences between different genders for each species, suggesting the gender effect on the *in vitro* metabolism of meisoindigo was negligible for rats, pigs and humans.

Table 3
The calculated *in vitro* $t_{1/2}$ and *in vitro* CL_{int} values (mean ± SD) of meisoindigo for the three species with different genders.

Species	Gender	*In vitro* $t_{1/2}$ (min)	*In vitro* CL_{int} (ml/min/kg)
Rat	Male	29.69 ± 1.11	84.12 ± 3.23
	Female	30.10 ± 0.46	82.92 ± 1.26
Pig	Male	35.93 ± 4.63	–
	Female	37.12 ± 4.28	–
Human	Male	22.27 ± 1.36	84.19 ± 5.13
	Female	23.01 ± 0.64	81.31 ± 2.30

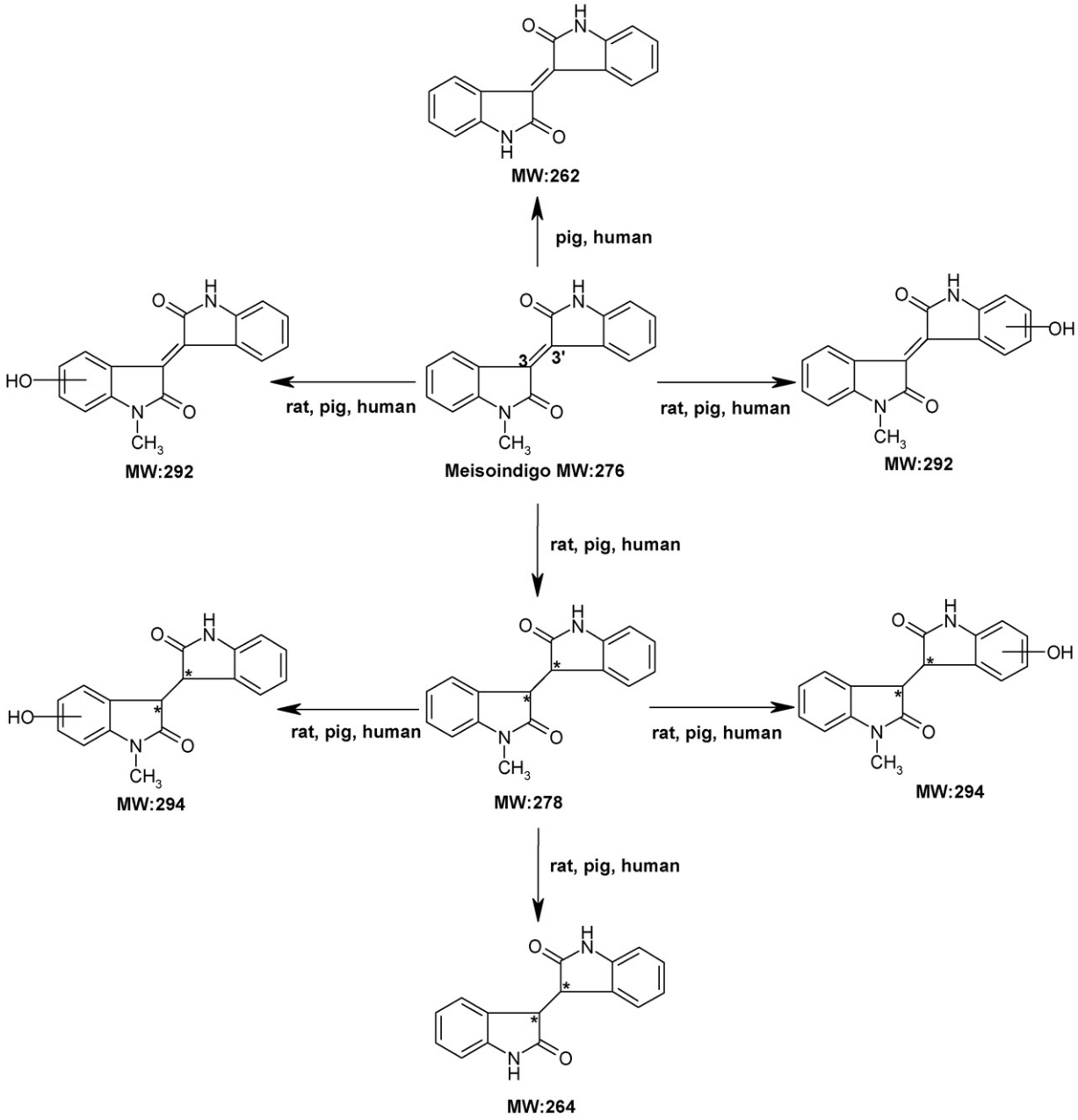

Fig. 5. Proposed metabolic pathway of meisoindigo in rat, pig, and human liver microsomes. Chiral centers are indicated with asterisks.

3.3. Metabolite formation

The formation of two major reductive metabolites of meisoindigo in both genders for rat, pig and human liver microsomes were plotted, respectively (data not shown). The metabolite formation profiles of M279-1 and M279-2 at different time points showed similar trends in each of the liver microsomes. All the curves did not start ascending from zero peak area at the time point of 0 min with the two reductive metabolites, indicating the existence of minute non-enzymatic reduction of meisoindigo in the control samples. Besides, M279-2 always showed higher abundance than M279-1, which further confirmed that reduction metabolism of meisoindigo was stereoselective. Formations of each of the other minor metabolites of meisoindigo (Table 2) varied with species and were determined as well in triplicate at eight time points between 5 and 90 min in gender-specific rat, pig and human liver microsomes, respectively (data not shown).

4. Discussion

This is the first comparative investigation of *in vitro* phase I interspecies metabolism of meisoindigo in rat, pig and human with different genders from both qualitative and quantitative aspects. In the present study, rats (rodent animals) were chosen because rats express two major cytochrome P450 isoforms that are oligomerically related to human CYP3A4, CYP3A1 and CYP3A2 [15]. Pigs (nonrodent animals) were chosen because CYP3A29 has been identified in the pig according to European Molecular Biology Laboratory/GenBank/DNA Data Bank of Japan databank submissions [16] as an ortholog of human CYP3A4. Furthermore, it has been reported that there are similarities between pig and human CYP450 metabolizing systems [17,18].

In terms of qualitative analysis, the *in vitro* metabolic pathways of meisoindigo in rat, pig and human liver microsomes were proposed as stereoselective reduction, stereoselective reduction

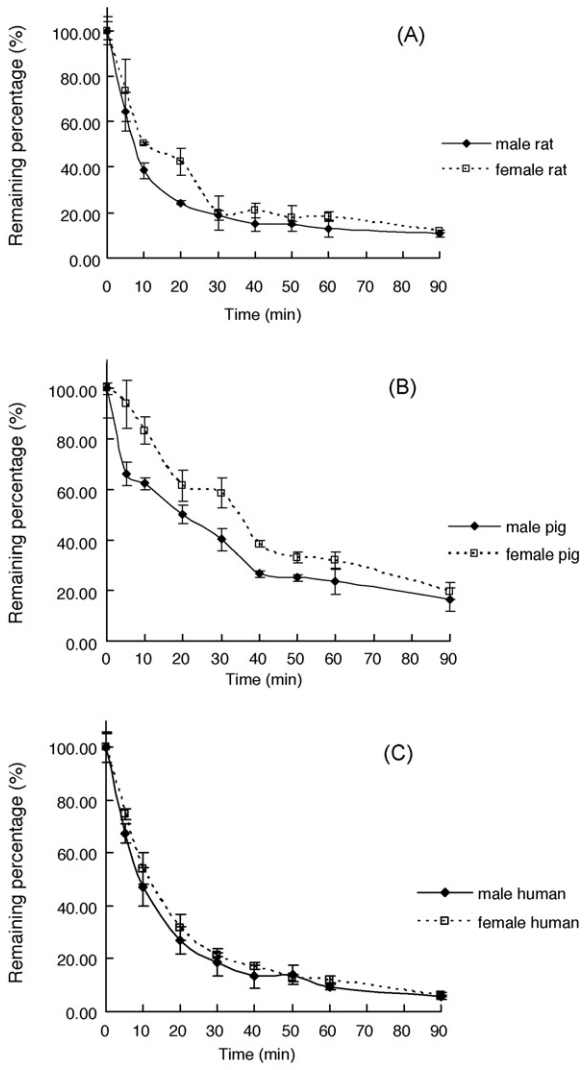

Fig. 6. Metabolic stability profiles for meisoindigo in liver microsomes: rat (A), pig (B), and human (C).

followed by N-demethylation, as well as both stereoselective and regioselective reduction followed by phenyl mono-oxidation, which were consistent with those in male rat liver microsomes reported previously [5]. Two more novel metabolic pathways were proposed as direct phenyl mono-oxidation in all of the three liver microsomes, as well as direct N-demethylation in only pig and human liver microsomes. From this point of view, pig might potentially be a better model than rat for the assessment of toxicological risks associated with meisoindigo metabolites, at least from a metabolic perspective. It was not clear that whether direct phenyl mono-oxidation was regioselective or not, whereas direct N-demethylation was definitely neither stereoselective nor regioselective since only one metabolite was likely to be formed.

On the other hand, metabolites generated from the respective processes of reduction, reduction followed by N-demethylation, and reduction followed by phenyl mono-oxidation metabolism of meisoindigo were more evident in rat liver microsomes than in the microsomes of the other two species. In contrast, direct phenyl mono-oxidation and direct N-demethylation metabolism of meisoindigo were more evident in pig liver microsomes than in rat and human microsomes. In addition, the two metabolites undergone reduction followed by phenyl mono-oxidation at positions 4, 5, 6 or 7 i.e. M295-6 (4.87 min) and M295-7 (5.05 min), as well as one metabolite undergone direct phenyl mono-oxidation i.e. M293-2 (5.08 min) were unique to the human liver microsome, suggesting that the correlation between the metabolism of meisoindigo in humans and these two preclinical animal species must be made with care.

In terms of semi-quantitative analysis, the metabolic stability and metabolite formation of meisoindigo in these three species were determined and plotted, respectively. The depletion method, first-order consumption of parent drug meisoindigo was monitored in liver microsomal incubations to yield *in vitro* $t_{1/2}$ values, assuming that the substrate concentration (1 μM) used is well below the Km value of all the important metabolizing enzymes involved in the metabolism of meisoindigo. The *in vitro* intrinsic clearance (CL_{int}) values of meisoindigo in gender-specific rat and human liver microsomes were calculated accordingly as well. Extrapolation of *in vivo* hepatic clearance from *in vitro* intrinsic clearance involved the use of equations describing the well-stirred or parallel tube liver models of *in vivo* hepatic clearance. One of the underlying assumptions is that oxidative microsomal metabolism is the predominant one [11]. However, the major metabolic pathway of meisoindigo is reduction, which does not meet this assumption. Thus, the extrapolation of *in vivo* hepatic clearance could not be performed.

In addition, statistical analysis showed that there were overall similarities in the metabolic stability profiles of meisoindigo in terms of amount of substrate remaining within 90 min of incubation among rat, pig and human. This result exhibited a good correlation in the *in vitro* metabolism of meisoindigo between human and these two preclinical animal species, thus providing adequate evidence for the prediction of *in vitro* metabolism of meisoindigo in human from those in rat and pig, as well as the decision of appropriate species for toxicology studies. It should be also noted that the unique metabolites which are only present in human rather than other preclinical animal species must be seriously taken into account in the process of the human metabolism prediction using other species. Furthermore, statistical analysis showed that there were overall similarities in the metabolic stability profiles of meisoindigo between different genders among the three species. These results could lead to a better understanding of the gender effect on metabolic profile of meisoindigo among the three species, and implied that it might not be necessary to adjust the dosing regimen of meisoindigo according to different patient genders for more effective and safer therapy of chronic myelogenous leukemia.

On the other hand, the subtle differences among species could not be fully revealed through the determination of the parent disappearance, which was conducted by monitoring the decrease of the parent drug from a high initial concentration and thus compromising the sensitivity of the measurement. In contrast, the metabolite formation was measured against the blank, and thus reliably provided meaningful information of relative kinetics comparison of each phase I metabolites of meisoindigo in the three species. Considering the signal to noise (S/N) ratios of some minor metabolites at certain time points were below 10 though above 3.3, only the formation profiles of the most significant and the most common reductive metabolites were discussed herein. It should be noted that the formation rates of the reductive metabolites were not shown in our study due to absence of the metabolite standards. Although the two reductive metabolites have been synthesized, it was found that the conversion of M279-1 to M279-2 was likely to take place especially in liquid state [5], which caused difficulty to determine the formation rates accurately.

In terms of the methodology adopted, the smaller particle size of UFLC and higher sensitivity of MRM jointly led to the successful detection of more reductive plus phenyl mono-oxidative metabolites at *m*/*z* 295 at trace levels with good resolution (Figs. 1 and 2), as well as new phenyl mono-oxidative metabolites at *m*/*z* 293

and one new N-demethyl metabolite at m/z 263, through filtering out unspecific responses in microsomal matrices. Co-eluting metabolites such as M295-6 (4.87 min), M295-14 (4.86 min) and M293-1 (4.87 min), were detected individually owing to the specificity of their respective MRM transitions. The UFLC coupled with MRM also enabled an overall better separation through a broader and shorter gradient elution program ranging from 5% to 95% within a total run time of 20 min.

However, the MRM in combination with EPI was unable to detect and identify unexpected metabolites as compared to the conventional full MS scan (EMS) in combination with MS/MS (EPI), if the MRM transitions only depended on the generation through the script in Analyst software to cover the unknown metabolites. This disadvantage was improved by addition of possible MRM transitions or removal of unlikely MRM transitions based on the knowledge of the metabolic predictions and the MS/MS fragmentation pattern prediction, as well as experimental results obtained by EMS in combination with EPI reported previously [5]. From another point of view, the pilot study showed that EMS spectra and UV chromatograms for the three species were similar while the minor metabolites were only observed in the rat, suggesting that the extent of metabolism in the rat was relative high and thus it was reasonable to search out most of the metabolites in the pig and human based on the MRM transitions obtained from the experiments with rat microsomes. In addition, MRM provided another dimension of relative kinetic information through simultaneous quantitative analysis of the parent drug disappearance and metabolite appearance as a function of time within one single sample injection. Therefore, integration of MRM with conventional metabolic profiling methodology enables a wide range of potential transitions to be targeted for metabolite detection and could be a powerful tool to provide more comprehensive metabolism information with regard to both qualitative and quantitative profiles of the drug.

Acknowledgement

This work was financially supported by the National University of Singapore Academic Research Fund R148-000-104-112.

References

[1] Cooperative Group of Clinical Therapy of Meisoindigo. Clinical studies of meisoindigo in the treatment of 134 patients with CML. Chin J Hematol 1988;9:135–7.
[2] Xiao ZJ, Hao YS, Liu BC, Qian LS. Indirubin and meisoindigo in the treatment of chronic myelogenous leukemia in China. Leuk Lymphoma 2002;43:1763–8.
[3] Xiao ZJ, Qian LS, Liu BC, Hao YS. Meisoindigo for the treatment of chronic myelogenous leukemia. Br J Haematol 2000;111:711–2.
[4] Peng Y, Wang MZ. Screening for in vitro metabolites of meisoindigo using RP-HPLC-DAD with gradient elution. Acta Pharmaceut Sin 1990;25:208–14.
[5] Huang M, Goh LT, Ho PC. Identification of stereoisomeric metabolites of meisoindigo in rat liver microsomes by achiral and chiral LC–MS/MS. Drug Metab Dispos 2008;36:2171–84.
[6] Shou WZ, Magis L, Li AC, Naidong W, Bryant MS. A novel approach to perform metabolite screening during the quantitative LC–MS/MS analyses of *in vitro* metabolic stability samples using a hybrid triple-quadrupole linear ion trap mass spectrometer. J Mass Spectrom 2005;40:1347–56.
[7] Chen Y, Monshouwer M, Fitch LW. Analytical tools and approaches for metabolite identification in early drug discovery. Pharm Res 2007;24:248–57.
[8] Gibson GG, Skett P. Techniques and experiments illustrating drug metabolism. In: Gibson GG, Skett P, editors. Introduction to drug metabolism. London: Blackie Academic and Professional; 1994. p. 240–2.
[9] Bradford MM. A rapid and sensitive method for the quantitation of microgram quantities of protein utilizing the principle of protein-dye binding. Anal Biochem 1976;72:248–54.
[10] Obach RS. Prediction of human clearance of twenty-nine drugs from hepatic microsomal intrinsic clearance data: an examination of in vitro half-life approach and nonspecific binding to microsomes. Drug Metab Dispos 1999;27:1350–9.
[11] Obach RS, Baxter JG, Liston TE, Silber BM, Jones BC, MacIntyre F, et al. The prediction of human pharmacokinetic parameters from preclinical and *in vitro* metabolism data. J Pharmacol Exp Ther 1997;283:46–58.
[12] Davies B, Morris T. Physiological parameters in laboratory animals and humans. Pharm Res 1993;10:1093–5.
[13] Houston JB. Utility of in vitro drug metabolism data in predicting in vivo metabolic clearance. Biochem Pharmacol 1994;47:1469–79.
[14] Iwatsubo T, Hirota N, Ooie T, Suzuki H, Shimada N, Chiba K, et al. Prediction of *in vivo* drug metabolism in the human liver from *in vitro* metabolism data. Pharmacol Ther 1997;73:147–71.
[15] Nelson DR, Koymans L, Kamataki T, Stegeman JJ, Feyereisen R, Waxman DJ, et al. P450 superfamily: update on new sequences, gene mapping, accession numbers and nomenclature. Pharmacogenetics 1996;6:1–42.
[16] Jurima-Romet M, Casley WL, Leblanc CA, Nowakowska M. Evidence for the catalysis of dextromethorphan *O*-demethylation by a CYP2D6-like enzyme in pig liver. Toxicol in Vitro 2000;14:253–63.
[17] Anzenbacher P, Anzerbacherova E, Zuber R, Soucek P, Guengerich FP. Pig and minipig cytochromes P450. Drug Metab Dispos 2002;30:100–2.
[18] Myers MJ, Farrell DE, Howard KD, Kawalek JC. Identification of multiple constitutive and inducible hepatic cytochrome P450 enzymes in market weight swine. Drug Metab Dispos 2001;29:908–15.